Memoirs of the School of Engineering, Okayama University, Vol. 18, No. 1, January 1984

Convergence Condition of Explicit Finite Element Method for Heat Transfer Problem

Takeo TANIGUCHI*, Takumi MATSUMOTO* & Kazuhiko MITSUOKA*

(Received December 28, 1983)

SYNOPSIS

The convergence condition of the explicit difference method for the heat transfer problem is aiready obtained. On the other hand, if the problem is formulated by using the weighted residual method for spatial axis, we have no tool to estimate the critical time-step width. In this paper, the estimation method is theoretically presented, and its propriety is examined through a number of numerical experiments.

1. INTRODUCTION

Heat Transfer Equation is the one which governs the heat transfer phenomenon, and in the field of Civil Engineering, many phenomena are govered by the same equation, for example, the seepage problem, the problem of the salt wedge in the ground water, the water pollution and the thermal stress in massive concrete. And, their solutions are desired.

The development of the digital computer in recent years has caused that of the numerical analysis, and, at present most of governing equations which present actual engineering problems can be approximately solved. These approximate solutions are mainly obtained by use of the Finite Difference Method (FDM) and the Weighted Residual Method (WRM) including the finite element method (FEM). Both of them express the solution of the governing equation at approximate nodal values located in space and time domain. Historically, the former is

* Department of Civil Engineering

firstly developed, and it is widely applied in many engineering field. But, at its application to actual problem we find many difficulties for locating node in space, for example the settlement of grid nodes, the treatment of the complicated boundary configuration, and the introduction of the boundary conditions and so on. The Weighted Residual Method which is lately developed is advantageous comparing to FDM, because most of the comlexities encountered at the application of FDM disappear in WRM. Therefore, in recent years the discretization of spatial axes is mainly done by use of WRM. On the other hand, the discretization along the time axis for most of governing equation is done by applying the FDM. The reason is that FDM can prepare a number of effective procedures and suitable one among them can be arbitrarily selected. Especially, for rather large scale problems the forward difference scheme is preferably used,[1] because the objective linear equations need not to be solved but variables are explicitly determined. In the case of using the explicit method along the time axis and also any finite difference scheme along the spatial axes, the conditional equation on the stability of the numerical solution has been made clear.[2] But in case that FEM is applied for the discretization of spatial axes and the forward difference scheme is used for that of the time axis, the stability condition of the numerical solution is not yet clarified.

In this paper, firstly the heat transfer equation is formulated by using the Galerkin method along the spatial axes and by the forward-differrence scheme along time axis. Successively, the stability condition of the numerical solution for this mixed type of equations is theoretically introduced by using "Brauer's Theorem", and we discuss the merits of using the mixed-type of formuration (for the heat transfer problem) comparing to the stability condition according to FDM. The results are examined through a number of numerical experiments, and we show that the mixed type formulation can not only make the discretization of spatial and time axes ease but also elongate the width of the time-step comparing to the one by use of only FDM.

2. THE THEORETICAL ESTIMATION OF THE CRITICAL TIME STEP WIDTH

2.1 The Mixed Use of The Finite Element Method and The Finite Difference Method

Let's express the heat transfer equation as

$$\frac{\partial^2 \phi}{\partial x^2} + \frac{\partial^2 \phi}{\partial y^2} = \frac{\partial \phi}{\partial t} \tag{2.1}$$

with the boundary condition of eq.(2.2) which is illustrated in Fig.2-2.

$$\left.\begin{aligned} \phi &= \bar{\phi} && \text{on } S_1 \\ \frac{\partial \phi}{\partial n} &= -h(\phi - v) && \text{on } S_2 \end{aligned}\right\} \tag{2.2}$$

,where h is the heat transfer coefficient and v is the value of ϕ out of the region.

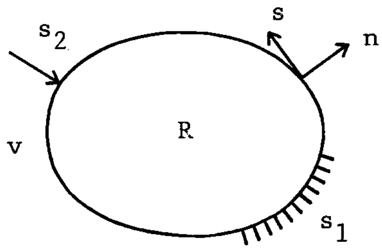

Fig.2-1 Boundary condition

Firstly we try discretizate eq.'s (2.1) and (2.2) by using WRM along the spatial axes and FDM along the time axis, respectively. At the application of WRM we fix the time axis, that is, the right-hand of eq.(2.1) can be expressed as

$$\frac{\partial \phi}{\partial t} = T \text{ (constant)} \tag{2.3}$$

Then, we may treat eq.(2.4) instead of eq.(2.1).

$$\frac{\partial^2 \phi}{\partial x^2} + \frac{\partial^2 \phi}{\partial y^2} - T = 0 \tag{2.4}$$

Application of The Galerkin Method on eq.(2.4) yields to [3)]

$$\iint \left(\frac{\partial^2 \phi}{\partial x^2} + \frac{\partial^2 \phi}{\partial y^2} - T \right) \delta\phi \, dxdy = \int_{S_2} \left\{ \frac{\partial \phi}{\partial n} + h(\phi - v) \right\} \delta\phi \, ds \tag{2.5}$$

Integration of eq.(2.5) gives following expression;

$$\iint\left\{\frac{\partial\phi}{\partial x}\frac{\partial\delta\phi}{\partial x}+\frac{\partial\phi}{\partial y}\frac{\partial\delta\Phi}{\partial y}\right\}dxdy+\iint T dxdy$$
$$=-\int_{s_2}h(\phi-v)\delta\phi ds \qquad (2.6)$$

Let's express above equation in matrix form. For this purpose we introduce eq.(2.7).[4]

$$\phi=[N]^T\{\Phi\} \qquad (2.7)$$

,where [N] is the shape function matrix and $\{\Phi\}$ is the node value vector of an element.

Introduction of eq.(2.7) into eq.(2.6) gives the following matrix expression.

$$\iint\left(\frac{\partial[N]}{\partial x}\frac{\partial[N]^T}{\partial x}+\frac{\partial[N]}{\partial y}\frac{\partial[N]^T}{\partial y}\right)dxdy\{\Phi\}+\iint[N]dxdy\ T$$
$$=-h\int_{s_2}[N][N]^T ds+h\int_{s_2}[N]ds\ v \qquad (2.8)$$

Now, we consider on the discretization along the time axis. Since the spatial axes and the time axis are discretizated separetely, we set T = {T} and replace {**T**} by

$$T=\frac{\{\Phi_i\}-\{\Phi_{i-1}\}}{\Delta t} \qquad (2.9)$$

,where Δt is the discretization width along the time axis and $\{\Phi_i\}$, $\{\Phi_{i-1}\}$ are the grid value vector at the i, i-1 time steps respectively.

Eq.(2.9) is introduced in eq.(2.10) and we obtain

$$\iint\left(\frac{\partial[N]}{\partial x}\frac{\partial[N]^T}{\partial x}+\frac{\partial[N]}{\partial y}\frac{\partial[N]^T}{\partial y}\right)dxdy\{\Phi_{i-1}\}$$
$$+\iint\frac{1}{\Delta t}[N]dxdy(\{\Phi_i\}-\{\Phi_{i-1}\})$$
$$=-h\int_{s_2}[N][N]^T ds\{\Phi_{i-1}\}+h\int_{s_2}[N]ds\ v \qquad (2.10)$$

Finally, eq.(2.10) is expressed as the matrix equation;

$$\mathbf{K}\Phi_{i-1}+\mathbf{C}(\Phi_i-\Phi_{i-1})=-\mathbf{B}_1\Phi_{i-1}+\mathbf{B}_2 \tag{2.11}$$

,where

$$\left.\begin{aligned}
&\mathbf{K}=\iint\left(\frac{\partial[N]}{\partial x}\frac{\partial[N]^T}{\partial x}+\frac{\partial[N]}{\partial y}\frac{\partial[N]^T}{\partial y}\right)dxdy\\
&\mathbf{C}=\iint\frac{1}{\Delta t}[N]dxdy\\
&\mathbf{B}_1=h\int_{s_2}[N][N]^T ds\\
&\mathbf{B}_2=h\int_{s_2}[N]ds\ v
\end{aligned}\right\} \tag{2.12}$$

That is, eq.(2.11) is equivalent to following equation whose solution vector, Φ_i, is directly obtained by introducing Φ_{i-1}.

$$\Phi_i=\mathbf{A}\Phi_{i-1}+\mathbf{B} \tag{2.13}$$

$$\left.\begin{aligned}
&,\text{where } \mathbf{A}=\mathbf{C}^{-1}(\mathbf{C}-\mathbf{K}-\mathbf{B}_1)\\
&\mathbf{B}=\mathbf{B}_2
\end{aligned}\right. \tag{2.14}$$

2.2 The Critical Time - Step Width

From eq.(2.14) we obtain following expression;

$$\Phi_i=\mathbf{A}^i\Phi_0+(\mathbf{I}-\mathbf{A})^{-1}(\mathbf{I}-\mathbf{A}^i)\mathbf{B} \tag{2.15}$$

,where Φ_i is the value of Φ at the i-th time step and Φ_0 is the initial value.

Eq.(2.15) clarifies that the convergence of Φ_i to a definite value, i.e. $(\mathbf{I}-\mathbf{A})^{-1}\mathbf{B}$, is wholly governed by the property of the matrix $\mathbf{A}$. If the maximum eigenvalue, λ_{max}, of $\mathbf{A}$ satisfies following relation, then above equation converges.[5]

$$|\lambda_{max}| \leqq 1 \tag{2.16}$$

Let's examine the maximam eigenvalue of the matrix **A** in eq.(2.13). From eq.(2.14)

$$\mathbf{A}=(\mathbf{I}-\mathbf{C}^{-1}\tilde{\mathbf{K}})$$

,where $\tilde{\mathbf{K}}=(\mathbf{K}-\mathbf{B}_1)$.

Then, the s-th row of **A** is explictly expressed as following;

$$[\Delta t\tilde{K}_{s,1},\Delta t\tilde{K}_{s,2},\cdots,\Delta t\tilde{K}_{s,s-1},1-\Delta t\tilde{K}_{s,s},\Delta t\tilde{K}_{s,s+1},\cdots,\Delta t\tilde{K}_{s,n}]$$

, because the matrix **C** is the diagonal one, and its s-th diagonal element is equal to $C_s/\Delta t$.

Here, we apply the Brauer's Theorem which shows the domain of the eigenvalues of any matrix.[6]

$$1-a_{ss}\Delta t-P_s\Delta t \leqq \lambda_{max} \leqq 1-a_{ss}\Delta t+P_s\Delta t \tag{2.17}$$

,where $a_{ss}=\tilde{K}_{s,s}$ and $P_s=\sum_{k=1}^{s-1}|\tilde{K}_{s,k}|+\sum_{k=s+1}^{n}|\tilde{K}_{s,k}|$

Assume that **A** is a convergence matrix. Then, its λ_{max} must be subject to the restrictions of eq.s (2.16) and (2.17).

Therefore,

$$-1 \leqq 1-a_{ss}\Delta t-P_s\Delta t \tag{2.18}$$

$$1 \geqq 1-a_{ss}\Delta t+P_s\Delta t \tag{2.19}$$

From eq.(2.18) we obtain

$$\Delta t \leqq \frac{2}{a_{ss}+P_s} \tag{2.20}$$

And, from eq.(2.19) we obtain

$$(-a_{ss}+P_s)\Delta t \leqq 0 \qquad (2.21)$$

Since $\Delta t \geqq 0$, eq(2.21) yields to

$$-a_{ss}+P_s \leqq 0 \qquad (2.22)$$

But in practice the case

$$a_{ss}+P_s > 0 \qquad (2.23)$$

exists.

This contradiction appears because λ_{max} is subject to the restrictions of eq.s (2.18) and (2.19). Therefore, the domain where the real eigenvalues locate should be expressed as following instead of eq.(2.17).

$$1-a_{ss}\Delta t-P_s\Delta t+\beta \leqq \lambda_{max} \leqq 1-a_{ss}\Delta t+P_s\Delta t-\alpha \qquad (2.24)$$

,where α and β are the positive values. Eq.(2.24) is explained by the illustration given in Fig.2-2.

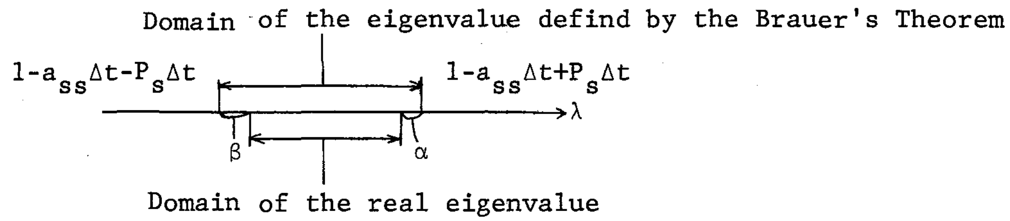

Fig.2-2 The domain of the eigenvalue

Here, we should notice that eq.(2.24) has no contradiction to the Brauer's Theorem, because the theorem can show only the maximum domain where all eigenvalues exist. Then, λ_{max} must be subject to the restrictions of eq.s (2.16) and (2.24), so we obtain

$$-1 \leqq 1-a_{ss}\Delta t-P_s\Delta t+\beta \qquad (2.25)$$

$$1 \geqq 1-a_{ss}\Delta t+P_s\Delta t-\alpha \qquad (2.26)$$

From eq.(2.25)

$$\Delta t \leqq \frac{2+\beta}{a_{ss}+P_s} \tag{2.27}$$

From eq.(2.26)

$$\Delta t \leqq \frac{\alpha}{-a_{ss}+P_s} \tag{2.28}$$

But, at present we have no information on the value of α and β. Therefore, we set $\beta=0$ and ignore eq.(2.28), and the critical time-step width is represented as

$$\Delta t \leqq \frac{2}{a_{ss}+P_s} \tag{2.29}$$

As far as Δt satisfies eq.(2.29), the calculation converges, and also eq.(2.28) is satisfied automatically. In this paper, above equation is used for the theoretical estimation of Δt_{cr}. Above consideration on the convergence condition of eq.(2.29) by use of the Brauer's Theorem results in that the condition is actually determined by the values of entries of **A**, as shown in eq.(2.29). Let the domain of our concern be as shown in Fig.2-1. Then, it is obvious that the critical value, Δt_{cr} of whole equation is determined by nodal points in R, on S_1 or on S_2. Let's denote the minimum values of Δt in R, on S_1 and on S_2 by $\Delta t_{cr}^{(1)}$, $\Delta t_{cr}^{(2)}$, $\Delta t_{cr}^{(3)}$, respectively. Then, the critical time-step, Δt_{cr}, for whole system is expressed as following,

$$\Delta t_{cr} = \min\left(\Delta t_{cr}^{(1)},\ \Delta t_{cr}^{(2)},\ \Delta t_{cr}^{(3)} \right) \tag{2.30}$$

We show that Δt_{cr} has no influence on the convergence condition as far as we use the explicit solution method.

Let's rewrite eq.(2,13) as following,

$$\begin{Bmatrix} \tilde{\Phi}_i \\ \Phi_{i,1} \end{Bmatrix} = \begin{bmatrix} \mathbb{A}_{11} & \mathbf{A}_{12} \\ \mathbb{A}_{21} & \mathbb{A}_{22} \end{bmatrix} \begin{Bmatrix} \tilde{\Phi}_{i-1} \\ \Phi_{i-1,1} \end{Bmatrix} + \begin{Bmatrix} \tilde{\mathbf{B}} \\ \mathbf{B}_1 \end{Bmatrix} \tag{2.31}$$

, where subscript "1" indicates the nodal value of S_1. Since $\Phi_{i,1} = \Phi_{i-1,1}$ ($= \Phi_1$), we may treat following expression instead of eq.(2,13).

$$\tilde{\Phi}_i = \mathbf{A}_{11}\tilde{\Phi}_{i-1} + \mathbf{A}_{22}\Phi_1 + \tilde{\mathbf{B}} \tag{2.32}$$

And, the convergence condition is governed only by the maximum eigenvalue of $\mathbf{A}_{11}$, which is the submatrix of $\mathbf{A}$. Then, we may treat eq.(2.33) instead of eq.(2.30).

$$\Delta t_{cr} = \min\ (\ \Delta t_{cr}^{(1)},\ \Delta t_{cr}^{(3)}\ ) \qquad (2,33)$$

But, we should notice that Δt_{cr} obtained from eq(2.33) can't give the true critical value, because in above theoretical consideration we set $\beta=0$ and ignore eq(2.28) and get eq(2.29).

In successive section the difference between the true critical and theoretical values are surveyed through a number of numerical experiments.

3. NUMERICAL EXPERIMENTS ON THE CRITICAL TIME - STEP WIDTH

In preceding section the critical time-step width, Δt_{cr}, is theoretically obtained by using the Brauer's Theorem, and the considerations on the estimation method clarified that the theoretical value of Δt_{cr} may be an underestimated one. That is, it is expected that the true critical value is larger than the estimated one.

In this section the extension of the estimated value of Δt_{cr} is measured through a number of numerical experiments. Eq.(2.33) for the estimation of Δt_{cr} clarifies that the critical time-step width is influenced by the physical, geometrical and topological properties which decide the values of entries in the coefficient matrix.

But the most important concern for the user of the mixed-type formuration as given in this paper is what kind of facters of the discretization procedures gives influences to Δt_{cr}. Finite element models used in this numerical experiments are as following;

The domain is a unit square area, i.e. $0 \leqq x \leqq 1$ and $0 \leqq y \leqq 1$, and the area is subdivided into N and M nodes located along x and y axes, respectively. All finite elements have the same property of constant strain, and only the central node of the region is heated. By using above finite element nodes we examine the influences of following factors to true Δt_{cr}.

1. The influence of the lengthes of the finite elements.
2. The influence of the different boundary conditions.
3. The influence of the conbination of several element lengthes.

Furthermore, by slight modification of above model we can examine following item;

4. The influence of the angle of finite elements.

The results obtained by the numerical experiments are as followings;

[Experiment 1] Uniformly subdivided model

The purpose of this experiment is to know the influence of the element-length on Δt_{cr}. The unit area is uniformly subdivided, and the lengthes of element is $\Delta x\{=1/(N-1)\}$ and $\Delta y\{=1/(M-1)\}$ along x and y axes, respectively. (See Fig.3-1)

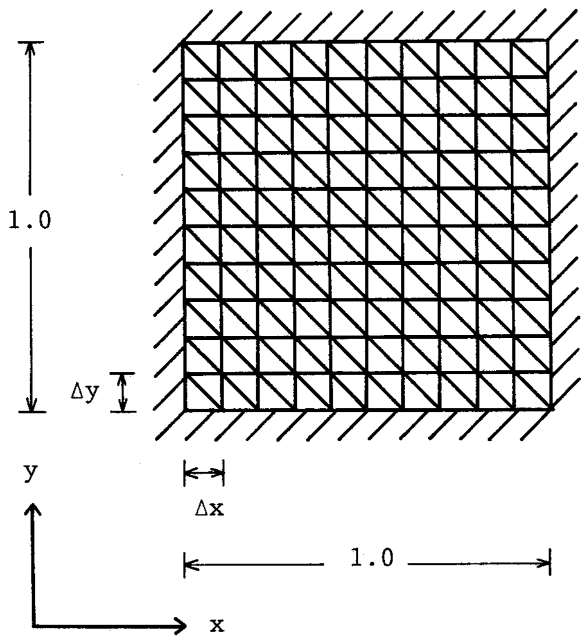

Fig.3-1 Uniformly subdivided model

All boundaries is s_1 type, because by this restriction the influence of the boundary condition is removed as mentiond in previous section. The theoretical value of Δt_{cr} is easily obtained by applying the Brauer's Theorem for an arbitrarily selected row in the coefficient matrix **A**.

$$1-4\left(\frac{\Delta t}{\Delta x^2}+\frac{\Delta t}{\Delta y^2}\right) \leqq \lambda_{max} \leqq 1 \tag{3.1}$$

,where Δx and Δy are the element lengthes along x and y axes, respectively. Since we have $|\lambda_{max}| \leqq 1$ for the numerical convergence, then the following critical value of the time-step width is obtained;

$$\Delta t_{cr} \leqq \frac{1}{2}\frac{\Delta x^2 \Delta y^2}{\Delta x^2+\Delta y^2} \tag{3.2}$$

Above condition is just same as the one which is obtained by FDM applied for spatial and time axes. The results of the numerical experiments are summarized in Table 3-1, and from the table we can remark following items;

1. The theoretical values of Δt_{cr} have good coincidence with the experimental values.
2. The extension of Δt_{cr} becomes large when both of Δx and Δy are enlarged at the same time.

This experiments result in that eq.(3.2) can give good estimation of the critical value of the time-step width for this case.

Table 3-1 The result of the numerical experiments

		0.025	0.050	0.100	0.167
0.025	E	1.561	-	-	-
	T	1.561			
0.050	E	2.500	6.249	-	-
	T	2.500	6.249		
0.100	E	2.940	10.27	25.66	-
	T	2.940	10.00	25.00	
0.167	E	3.093	11.77	37.90	71.13
	T	3.093	11.46	36.80	69.66

($\times 10^{-4}$)

Note; E and T means the experimental and theoretical values, respectively.

[Experiment 2] Irregularly subdivided model

The aim of this experiment is to know the influence of the different element lengthes set in a model. For this purpose a unit square with only s_1-type boundary condition is irregularly subdivided along x-axis and uniformly along y-axis. The loading condition is just same as the one of the experiment 1. The model used in this experiment is illustrated in Fig.3-2, and the results are summarized in Fig.3-3,3-4 and 3-5.

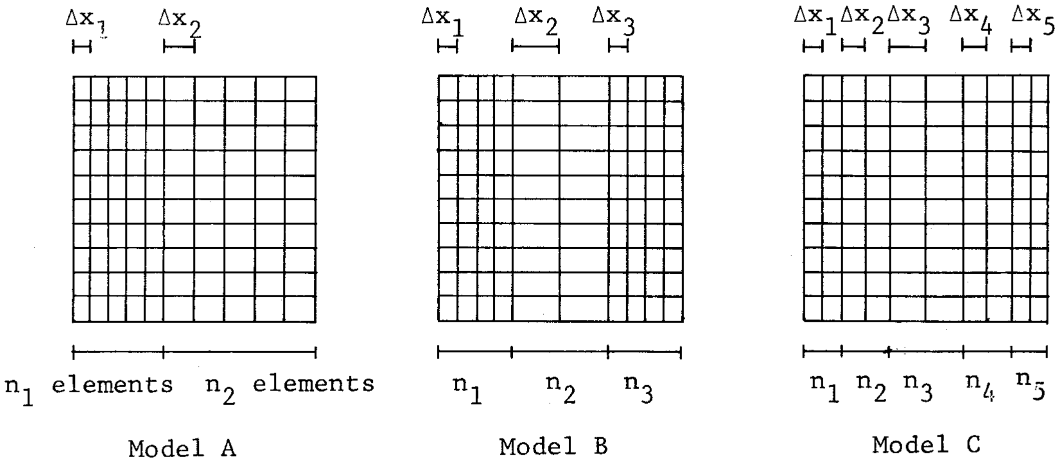

Fig.3-2 Models for the experiments

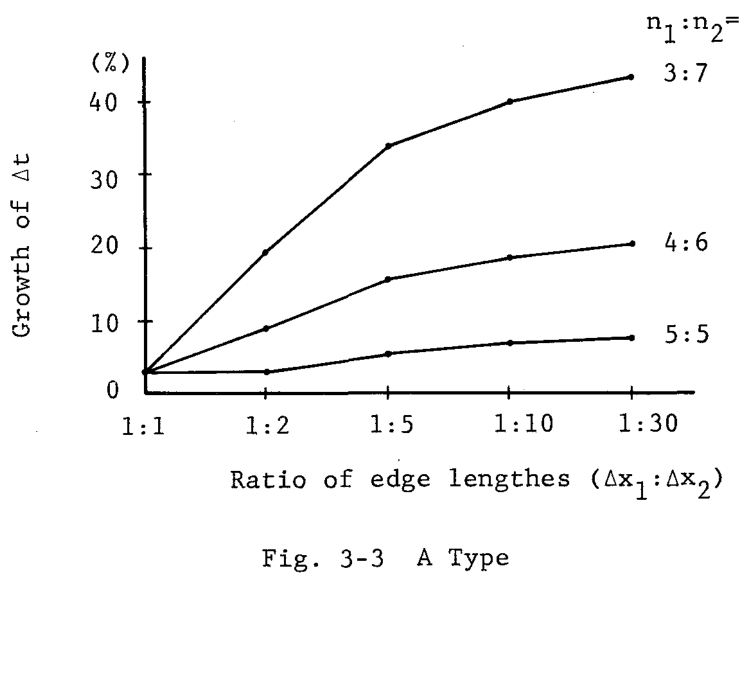

Fig. 3-3 A Type

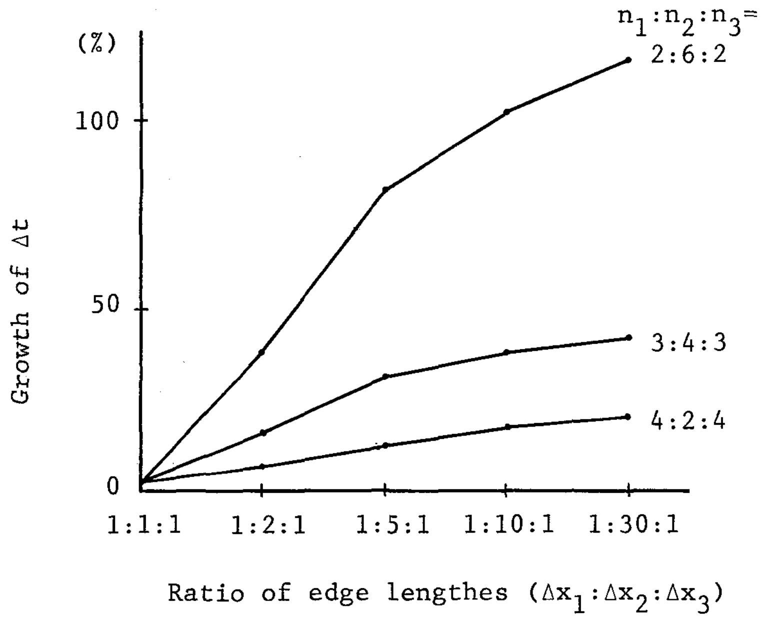

Fig. 3-4 B Type

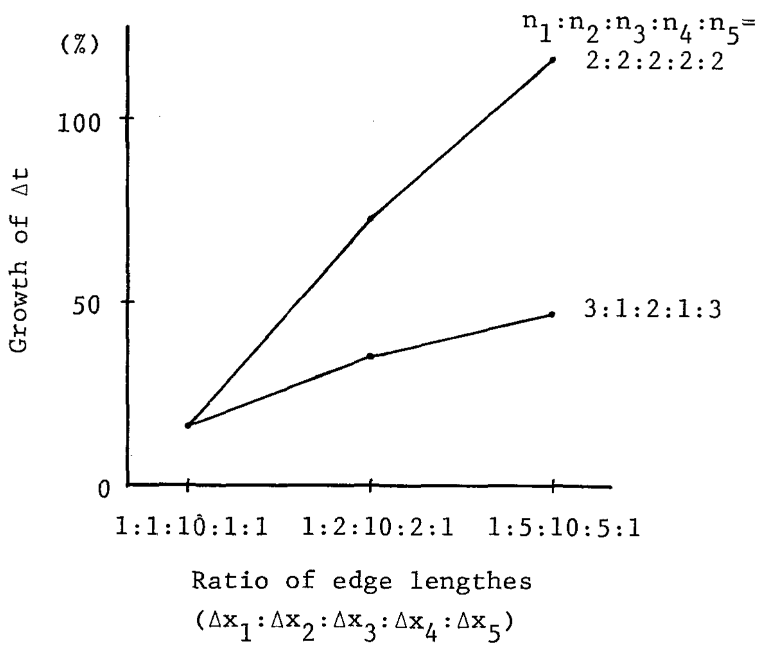

Fig. 3-5 C Type

The theoretical value given in the figure for the comparison are obtained by applying the Brauer's Theorem for the row, which corresponds to the node surrounded by the smallest elements, in the coefficient matrix **A**. Then, we obtain

$$1-4\left(\frac{\Delta t}{\Delta x_s^{\,2}}+\frac{\Delta t}{\Delta y_s^{\,2}}\right) \leqq \lambda_{max} \leqq 1 \qquad (3,3)$$

,where Δx_s and Δy_s are the smallest element lengthes, which surround the node, along x and y axes, respectively.

Since we have $|\ \lambda_{max}\ | \leqq 1$ for the numerical convergence, then the following critical value of the time-step width is obtained;

$$\Delta t_{cr} \leqq \frac{\Delta x_s^{\,2}\Delta y_s^{\,2}}{\Delta x_s^{\,2}+\Delta y_s^{\,2}} \qquad (3.4)$$

The result of the experiments are summarized as followings;

(1) A node surrounded by finite elements with the smallest element length governs the critical value of Δt as it is expected from the theoretical consideration.

(2) The number of finite elements with the largest edge length gives influence to Δt_{cr}, and their location also gives influence to the value. That is, if they are located at the central area of the domain, then we may expect that true critical value of Δt is larger than the theoretical evaluation.

(3) The tendency of the increasing of observed values of Δt_{cr} comparing to its theoretical value is strengthened as the domain is discretizated irregularly.

[Experiment 3] Angle of triangular finite element

For this numerical experiment the domain is slightly modified and we treat a parallelogram as shown in Fig.3-6 instead of a square area.

For this modification we consider two types of parallelograms (A and B shown in Fig.3-6), and both cases are used for the experiments. Their surrounding edges are restricted to be s_1-boundary condition. Theoretical values of Δt_{cr} for this experiment are evaluates as followings;

(1) The acute-angled triangular elements (See.Fig.3-7)
The entries of an arbitrarily selected row in the coefficient matrix **A** is as following;

$$[\ \cdots\ \frac{L_1{}^2+L_2{}^2-L_3{}^2}{8\Delta^2}\Delta t\ \cdots\ \frac{-L_1{}^2+L_2{}^2+L_3{}^2}{8\Delta^2}\Delta t\ \cdots$$

$$\frac{L_1{}^2-L_2{}^2+L_3{}^2}{8\Delta^2}\Delta t\ \cdots\ 1-\frac{L_1{}^2+L_2{}^2+L_3{}^2}{4\Delta^2}\Delta t\ \cdots\ \frac{L_1{}^2-L_2{}^2+L_3{}^2}{8\Delta^2}\Delta t$$

$$\cdots\ \frac{-L_1{}^2+L_2{}^2+L_3{}^2}{8\Delta^2}\Delta t\ \cdots\ \frac{L_1{}^2+L_2{}^2-L_3{}^2}{8\Delta^2}\Delta t\ \cdots\ ]$$

, where L_1, L_2, L_3 are the length of three edges of the trianglar element shown in Fig.3-5 and Δ is the area.

Then, the Brauer's Theorem gives following expression;

$$1-\frac{L_1{}^2+L_2{}^2+L_3{}^2}{2\Delta^2}\Delta t \leqq \lambda_{max} \leqq 1 \qquad (3.5)$$

Consider that λ_{max} must locate between -1 and 1, then we obtain following stability condition for Δt_{cr};

$$\Delta t_{cr} \leqq \frac{4\Delta^2}{L_1{}^2+L_2{}^2+L_3{}^2} \qquad (3.6)$$

(2) The obtuse-angled triangular elements (See.Fig.3-8)
The entries of a row in the coefficient matrix **A** is the same one of the first case. The application of the Brauer's Theorem yield to be

$$|\ \lambda_{max} - (\ 1-\frac{L_1{}^2+L_2{}^2+L_3{}^2}{4\Delta^2}\Delta t\ )\ | \leqq \frac{-L_1{}^2+3L_2{}^2-L_3{}^2}{4\Delta^2}\Delta t \qquad (3.7)$$

,where L_1, L_2 and L_3 are lengthes of three edges of the triangle element and we assume that L_2 is the longest one among them.

The same procedure presented in case (1) follows to

$$\Delta t_{cr} \leqq \frac{2\Delta^2}{L_2{}^2} \qquad (3.8)$$

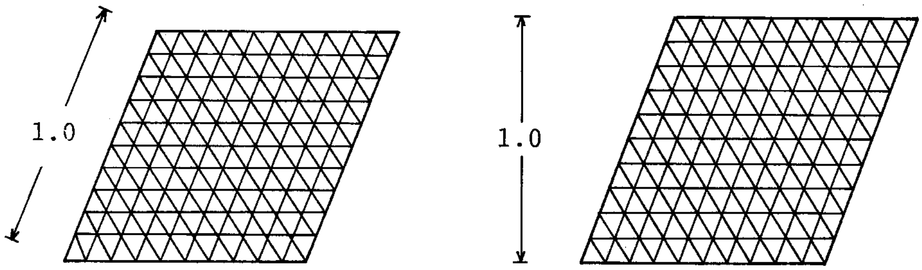

A

The edge lengthes
are invariable.

B

The area of the region
is invariable.

Fig. 3-6 The parallelogram domain

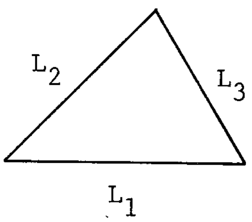

Fig.3-7

The acute-angled
triangular element

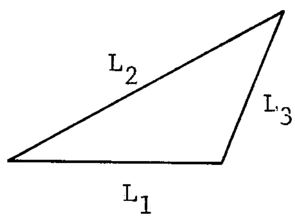

Fig.3-8

The obtuse-angled
triangular element

Now, we show the results of the numerical experiments.
(See.Fig.3-9)

From these experiments we can notice following items;

(1) The increasing of the observed value of Δt_{cr} to the theoretical one is maximized at $\theta=60°$ in both cases, A and B, and the growth of Δt for the thoretical value reaches round 30%.

(2) For case B with $\theta<45°$ we can't expect the increasing of the critical time-step width comparing to the theoretical one.

(3) From the first item the discretization using regular triangle

finite elements is preferable from the view point of the numerical stability, because increasing of Δt_{cr} is expected.

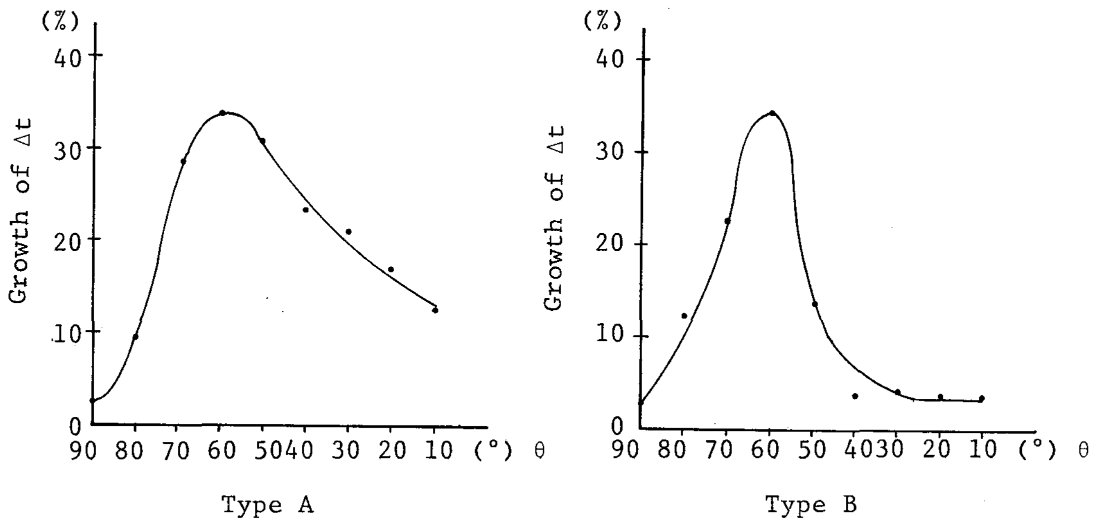

Fig.3-9 The results of Experiment 3

[Experiment 4] Boundary condition

In the mixed-type formulation given in section 2 we consider two type of boundary conditions, i.e. S_1 and S_2. The consideration in previous section clarified that s_1-condition gives no influence to the numerical stability. Therefore, in this experiment we consider the influence of s_2-boundary condition, that is

$$\frac{\partial \phi}{\partial n} = -h(\phi - v) \tag{3.9}$$

,where h is the heat transfer coefficient and v is the value of ϕ out of the region.

For this purpose the square area is regularly subdivided, and for all nodes on boundary above boundary condition is applied. This boundary condition is introduced in the coefficient matrix as the matrix $\mathbf{B}_1$ and $\mathbf{B}_2$ in eq.(2.12). In this experiment we must examine the propriety of eq.(2.33). $\Delta t_{cr}^{(1)}$ shown in eq.(2.33) is obtaind as eq.(3.2). $\Delta t_{cr}^{(3)}$ is obtained as following.

The entries of the row, which correspond the node on s_2, are as followings;

$$\left[\frac{3}{2}\frac{\Delta t}{\Delta x^2} \cdots \frac{3}{2}\frac{\Delta t}{\Delta y^2} - \frac{1}{2}h\frac{\Delta t}{\ell} \quad 1-\left(3\frac{1}{\Delta y^2}+\frac{3}{2}\frac{1}{\Delta x^2}+h\frac{2}{\ell}\right)\Delta t \quad \frac{3}{2}\frac{\Delta t}{\Delta y^2} - \frac{1}{2}h\frac{\Delta t}{\ell} \cdots \right]$$

,where ℓ is the element length on s_2.

Then, the Brauer's Theorem gives following expression;

$$1-3\frac{\Delta t}{\Delta x^2}-6\frac{\Delta t}{\Delta y^2}-h\frac{\Delta t}{\ell} \leqq \lambda_{max} \leqq 1-3h\frac{\Delta t}{\ell} \tag{3.10}$$

Consider that λ_{max} must locate between -1 and 1, then we obtain

$$\Delta t \leqq \frac{2}{3}\frac{1}{\dfrac{2}{\Delta x^2}+\dfrac{1}{\Delta y^2}+\dfrac{1}{3}h\dfrac{1}{\ell}} \tag{3.11}$$

$$3\,h\frac{\Delta t}{\ell} \geqq 0 \tag{3.12}$$

In case $h>0$, eq.(3.12) is absolutely satistied. So we obtain

$$\Delta t_{cr}^{(3)} \leqq \frac{2}{3}\frac{1}{\dfrac{2}{\Delta x^2}+\dfrac{1}{\Delta y^2}+\dfrac{1}{3}h\dfrac{1}{\ell}} \tag{3.13}$$

Table 3-2 The result of Experiment 4

h	$\Delta t_{cr}^{(1)}$	$\Delta t_{cr}^{(3)}$	the real Δt_{cr}
0.1	0.00250	0.00221	0.00249
1.0	0.00250	0.00219	0.00247
10.0	0.00250	0.00200	0.00224
100.0	0.00250	0.00105	0.00125

The results are summarized in Table 3-2, and the table indicate following items;

(1) The physical value "h" gives influence to Δt_{cr}.

(2) The more the physical value "h" increase, the bigger the real Δt_{cr} is influenced by $\Delta t_{cr}^{(3)}$, that is, it is clarified the boundary condition shown in eq.(3.9) influence the convergence strongly.

4. CONCLUDING REMARKS

In this paper we presented the discretization method of the Heat Transfer Equation by using the finite element method in spatial axes and the explicit difference scheme in time axis, and the convergence condition of above explicit equation is surveyed theoretically and experiamentally. The thoretical approach could give several convergence conditions by applying the Brauer's Theorem, and through numerical experiments the propriety of proposed convergence conditions is examined. At the same time, it was also remarked that the critical time-step width by proposed method is underestimated one, and that the difference between the true critical width is governed by edge-length, angle of triangular finite elements, their rearrangement in the problem area and boundary condition. The authors could clarify that this difference is caused by the reduction process of the theoretical estimation method using the Brauer's Thorem. Generally speaking, the smallest finite element governs the critical time-step width, Δt_{cr}, except the boundary condition, and for the numerical stability the finite element model should consist of only regular triangular meshes.

References

1). M.Yagawa,"The Introduction of the Finite Element Method in the Flow and the Heat Transfer Problems", Baifukan, (1983), 1-6

2). Gordon D. Smith,"Numerical Solution of Partial Differntial Equations", Scinece-Sha, (1978), 63-67

3). J.J. Connor & C.A. Brebbia,"Finite Element Techniques For Fluid Flow", Science-Sha, (1979), 41-51

4). Ditto of 1) , 103-108

5). R.S.Varga,"Matrix Iterative Analysis", Prentice-Hall, (1962), 1-15

6) Ditto of 2) , 68-70